Military Technical College
Kobry El-Kobbah,
Cairo, Egypt.

18th International Conference on Applied Mechanics and Mechanical Engineering.

THERMAL ANALYSIS OF THE ISCC POWER PLANT IN KURAYMAT, EGYPT

A. Temraz[1], A. Rashad[2], A. Elweteedy[2] and K. Elshazly[3]

ABSTRACT

Integrated Solar Combined-Cycle (ISCC) technology combines the benefits of solar energy with the benefits of a combined cycle. The solar resource partially substitutes the fossil fuel. In this paper, a thermodynamic exergy analysis of the integrated solar combined cycle power plant in Egypt was implemented. The data is taken from the design documentations of the plant as well as the plant records. Exergy-based performance analysis based on the second law of thermodynamics overcomes the limit of studying the system based on the first law of thermodynamics. It assesses the magnitude of exergy destruction in each part of the system. The plant is a 135 MWe hybrid power plant composed of a combined cycle and a 20 MWe solar thermal plant. Exergy destruction throughout the plant is quantified and illustrated using an exergy flow diagram. The exergitic efficiency of each component of the ISCC is calculated. The results showed that the overall thermal efficiency and the 2nd law efficiency of the ISCC accounted for 32% and 40.8%, respectively. Also, it was revealed that the combustion chamber and the solar field represent the sites of the highest exergy destruction in the ISCC (34 % and 42.1% respectively). The sources of the exergy destruction in the combustion chamber and the solar field are discussed in order to identify the possibility to enhance the performance of the components of major exergy destruction.

KEYWORDS

Parabolic Trough Collector (PTC), Integrated Solar Combined-Cycle (ISCC), Solar energy, Energy, Exergy, Concentrated Solar Power (CSP), Power Plant.

---

[1] Egyptian Armed Forces. Corresponding author; Email: aymantemraz@mtc.edu.eg.
[2] Egyptian Armed Forces.
[3] Professor, Department of Mechanical Power Engineering, Faculty of Engineering-Shoubra, Benha University, Egypt.

NOMENCLATURE

A	Area [m^2].	$\dot{Q}$	Heat flow rate [kW]
h	Specific enthalpy [J/kg]	$\dot{Q}_{inc}$	Rate of heat addition to the ISCC from the solar field [kW]
H_v	Fuel heating value [kJ/kg]	s	Specific entropy [kJ/kg.K]
HL_{Rec}	Heat loss from the receiver, per unit Area [W/m^2]	T	Temperature [K].
$\dot{I}$	Rate of exergy destruction [kW]	$\dot{W}$	Power output [kW]
L	Length [m]	$\dot{W}_{net,out}$	Net power output of the power plant [kW]
$\dot{m}$	Mass flow rate [kg/s]	$\dot{X}_{cycle,in}$	Total rate of exergy input to the power plant [kW]
$N_{collectors}$	Number of the solar field collectors	$\dot{X}_a$	Rate of exergy of the air after the compressor [kW]
$\dot{X}_b$	Rate of exergy of the exhaust gases after the combustor [kW]	$\dot{X}_{heat}$	Rate of exergy transfer by heat [kW]
$\dot{X}_c$	Rate of exergy of the exhaust gases after the gas turbine [kW]	$\dot{X}_{work}$	Rate of exergy transfer by work [kW]

Greek Symbols

θ	Incidence angle [degree]	ζ	The ratio of chemical exergy and the net calorific value [-]
η	Efficiency [-].	Ψ	Specific exergy transfer [kJ/kg]

Subscripts

amb	Ambient.	i	Inlet.
av	Average.	inc	Incidence.
CP	Condensate pump.	o	the dead state.
e	Exit.	SF	Solar field.
elec	Electric.	ST	Steam turbine.
FWP	Feed water pump.	s	Source.
GT	Gas turbine.		

Abbreviations

CC	Combustion Chamber	HTF	Heat Transfer Fluid
CSP	Concentrated Solar Power	ISCC	Integrated Solar Combined Cycle

DNI	Direct Normal Irradiance	ISCCS	Integrated Solar Combined Cycle System
GTCC	Gas Turbine Combined Cycle	NGCC	Natural Gas Combined Cycle
HCE	Heat Collection Element	PTC	Parabolic Trough Collector
HRSG	heat recovery steam generator	ST	Steam Turbine

INTRODUCTION

Since CSP plants use steam to produce energy, in a similar manner to conventional steam power plants. The key difference is that CSP plants use emission-free, clean solar radiation to produce heat instead of fossil or nuclear fuels.

The receiver, the key component of a CSP plant, has a decisive influence on the overall efficiency of the plant. It must show high solar absorptance as well as low thermal emittance. Today, solar thermal power plants based on parabolic troughs represent the only solar power plant technology tested on a commercial basis. Therefore, they are promising candidates for providing a significant contribution to carbon dioxide mitigation [1].

However, for a variety of economic reasons, no new parabolic trough power plants have been built from 1990 to 2000. Due to the decision of the Global Environment Facility, in 2000, to provide grants for four Integrated Solar Combined Cycle (ISCC) power plants in India, Egypt, Morocco and Mexico, interest in this kind of power stations increased again [2].

Integrated Solar Combined Cycle System (ISCCS) proposed as a means of integrating a parabolic trough solar plant with modern combined cycle power plants. An integrated plant consists of a conventional combined cycle plant, a solar collector field, and a solar steam generator. In this kind of power plants (ISCC), the most efficient method for converting solar thermal energy to electric energy is to withdraw feed water from the heat recovery steam generator (HRSG) downstream of economizer, produce high-pressure saturated steam using solar energy, and return the steam to the HRSG for superheating by the gas turbine exhaust [3].

Baghernejad and Yaghoubi [4] carried out energy and exergy analysis for the solar field and combined cycle to analyze the Integrated Solar Combined Cycle in Yazd, Iran using design plant data. The results showed that the causes of exergy destruction in the plant include losses in the combustor, collector, heat exchangers, pump and turbines which account for 29.62, 8.69, 9.11 and 8% of the total exergy input to the plant, respectively. The values of energy and exergy efficiencies for the ISCCS are found to be 46.17% and 45.6%, respectively. These efficiencies are higher than a simple combined cycle power plant without solar contribution and also Rankine cycle power plants with parabolic trough technology. Behar et al. [3] simulated the performance of the first ISCC in Algeria, under Hassi R'mel climate conditions. The results showed that the output power increased from 134 MW to 157 MW and the thermal efficiency was increased from 57.5 to 67 %.

As a result of the current survey, the present work will be done to study the ISCC power plant in Egypt under Kuraymat conditions in details. The study will be focused on the exergy analysis.

PLANT DESCRIPTION

The plant is located in Kuraymat, about 87 km South of Cairo, Capital of Egypt. The site is located on the eastern side of the Nile River at northern latitude of 29° 16' and eastern longitude of 31° 15'. The construction of the ISCC Kuraymat power plant started in January 2008 and reached commercial operation as a whole at the end of June 2011 [2]. The plant in Kuraymat of approximately 135 MW total power capacity comprises a combined cycle field with a power of 115 MW and a solar field with an electrical output of 20 MW [5]. The integration of a GTCC with the solar field ensures that the hybrid delivers the required electricity contribution to the grid regardless of solar radiation conditions.

Solar Field

The solar field comprises parallel rows of Solar Collector Arrays and typical glass mirrors of 20 MW installed capacity. The solar field comprises 40 loops and each loop having four SKAL-ET 150 parabolic trough collectors. The total aperture of one collector is 817.15 m². The solar collectors are 160 forming 40 loops covering 130,800 m^2.

The solar heat transfer from the solar field collectors (PTCs) to the steam cycle is done by the HTF (heat transfer fluid) system. The HTF is Therminol VP-1 from Solutia (Ultra-high-temperature, liquid/vapor phase fluid) operates between 12° to 400°C (54° to 750°F) [6],[7]. The HTF system is designed for a HTF mass flow of 250 kg/s at 100% load. Hot HTF returning from the solar field at 393 °C is pumped through the solar heat exchanger. The HTF leaves the solar heat exchanger at 293 °C and is pumped back into the solar field.

Table 1 summarized the solar field design parameters. The design thermal power of the Solar Island is reached for DNI values between 700 and 800 W/m² depending on incident angle and status of the solar field (Number of loops in operation, tracking accuracy, mirror reflectivity etc.).

Table 1. The solar field design parameters [5],[8],[9].

Solar Field operation parameters	Unit	Value
Solar Field total Aperture Area	m²	130800
Number of Collectors	N°	160
Number of Collector Loops	N°	40
Design Irradiation	W/m²	700
Maximum Solar Field Thermal Power Output	MW	61
HTF Output Temperature	°C	393
HTF Input Temperature	°C	293

Combined Cycle

The Combined Cycle Island consists of one gas turbine, one heat recovery steam generator (HRSG), one steam turbine, solar heat exchangers plus all associated control and balance of plant equipment and installations.

The plant includes one GE type MS6001FA heavy-duty gas turbine with a generator of a rated electric power output of 70 MW at 20℃ ambient dry bulb temperature. The gas turbine combusts about 4.7 kg of natural gas per second and therefore require about 200 kg of combustion air per second [9].

At rated conditions of the gas turbine full load operation, the heat recovery steam generator receives about 206 kg/s flue gas from the gas turbine at temperatures of about 600℃. The flue gas leaves the HRSG at about 100℃.

The HRSG steam system design includes two low-pressure economizer, low-pressure evaporator, low-pressure steam drum and low-pressure super-heater for feed off the steam turbine low-pressure section, three high-pressure economizer, high-pressure evaporator, high-pressure steam drum and two high-pressure super-heater for feed of the high-pressure section of the steam turbine as shown in Fig. 1.

The ISCC Kuraymat includes a Siemens SST 900 series single casing, horizontally split condensing type steam turbine with a generator. At rated conditions of the gas turbine and HRSG full load operation, solar heat input of 50 MW and 20℃ ambient dry bulb temperature the steam turbine generator output is about 65 MW. The turbine has a high-pressure section that receives steam from the high-pressure super-heaters and a low-pressure section that receives steam from the low-pressure super-heaters and the high-pressure turbine section.

THERMODYNAMIC ANALYSIS

The ISCC is evaluated assuming steady-state operation, with no accounting for thermal capacitance. This assumption works fairly well through the majority of the operating day but creates some problems in the morning when the solar field is warming up.

Energy Balance

The net rate of heat input to the ISCC is given by:

$$\dot{Q}_{ISCC,in} = \dot{Q}_{fuel} + \dot{Q}_{inc} \tag{1}$$

where,

$$\dot{Q}_{fuel} = \dot{m}_{fuel} * H_v \tag{2}$$

$$\dot{Q}_{inc} = DNI * A_{SF} \tag{3}$$

The electric power output of the ISCC is given by:

$$\dot{W}_{elec,ISCC} = \dot{W}_{elec,GT} + \dot{W}_{elec,ST} \tag{4}$$

As a result, the overall efficiency of the plant is:

$$\eta_{I,cycle} = \frac{\dot{W}_{elec,ISCC}}{\dot{Q}_{ISCC,in}} \tag{5}$$

Exergy Efficiencies

There are two different approaches are generally used to calculate the exergy efficiency, one is called brute force, while the other is called functional which is defined as following [4]:

- Brute force exergy efficiency for any system is defined as the ratio between the sum of all output exergy terms and the sum of all input exergy terms.
- Functional exergy efficiency for any system is defined as the ratio between the exergy associated with the desired energy output and the exergy associated with the energy expended to achieve the desired output.

The brute force form of exergy efficiency is used in this paper. The brute force form requires accuracy and an explicit definition of each input and output exergy terms before calculate the exergy efficiency. The input exergy terms of this cycle represent the chemical exergy of the fuel, natural gas, and the exergy associated with the solar thermal energy input, solar power input.

So, the 2nd law efficiency (exergetic efficiency) is given by:

$$\eta_{II} = \frac{Exergy\ output}{Exergy\ input}$$

The net exergy transfer by heat ($\dot{X}_{heat}$) at temperature T_s is given by

$$\dot{X}_{heat} = \sum (1 - \frac{T_0}{T_s})\dot{Q}_s \tag{6}$$

And the specific exergy is given by:

$$\Psi = (h - h_0) - T_0(s - s_0) \tag{7}$$

Then the total exergy rate associated with a fluid stream becomes

$$\dot{X} = \dot{m} * \Psi = \dot{m}[(h - h_0) - T_0(s - s_0)] \tag{8}$$

For a steady state operation, the exergy destruction and the 2nd law efficiency of different components of the ISCC (from Fig. 1) are defined as shown in Table 2.

Fuel exergy definition

The fuel chemical exergy per unit time [kW]

$$\dot{X}_{fuel} = \zeta * \dot{Q}_{fuel} \tag{9}$$

where, ζ = ratio of chemical exergy and the net calorific value [-] which equal 1.04 for natural gas [11].

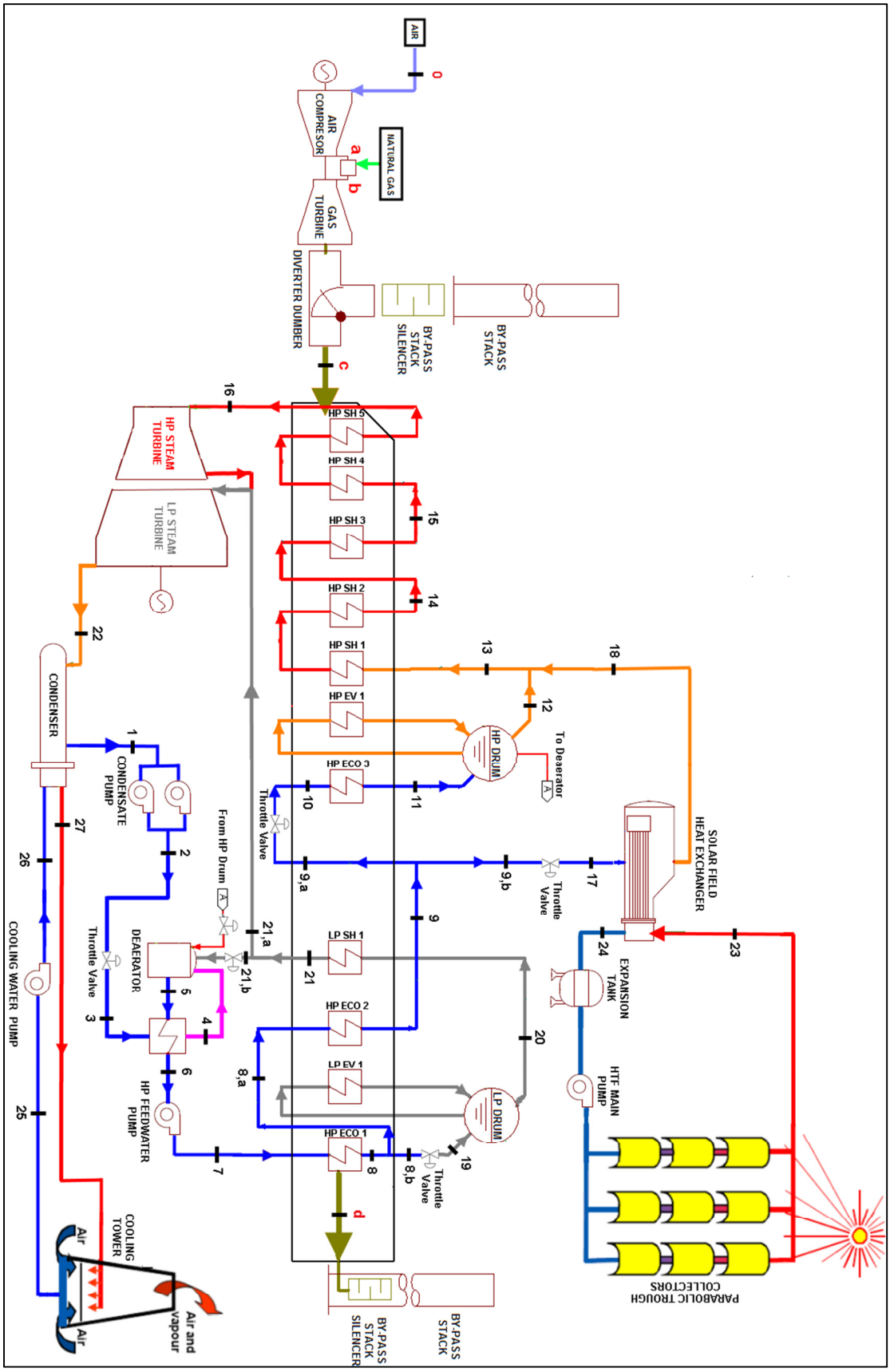

Fig. 1. Flow Diagram of ISCC in Kuraymat, Egypt with state points illustration.

Table 2. Definitions of the exergy destruction and the 2nd Law efficiency [10].

Components	Exergy destruction	2nd Law Efficiency (η_{II})
Pumps	$\dot{I}_{pump} = \dot{X}_{in} - \dot{X}_{out} + \dot{W}_{pump}$	$\eta_{II,pump} = 1 - \frac{\dot{I}_{pump}}{\dot{W}_{pump}}$
Heaters	$\dot{I}_{heater} = \dot{X}_{in} - \dot{X}_{out}$	$\eta_{II,heater} = 1 - \frac{\dot{I}_{heater}}{\dot{X}_{in}}$
Turbine	$\dot{I}_{turbine} = \dot{X}_{in} - \dot{X}_{out} - \dot{W}_{turbine}$	$\eta_{II,turbine} = 1 - \frac{\dot{I}_{turbine}}{\dot{X}_{in} - \dot{X}_{out}}$
Condenser	$\dot{I}_{condenser} = \dot{X}_{in} - \dot{X}_{out}$	$\eta_{II,condenser} = \frac{\dot{X}_{out}}{\dot{X}_{in}}$
Cycle	$\dot{I}_{cycle} = \sum_{all\ components} \dot{I}$	$\eta_{II,cycle} = \frac{\dot{W}_{net,out}}{\dot{X}_{cycle,in}}$

Solar field subsystem

The solar thermal heat input from HTF ($\dot{Q}_{\mathrm{HTF}}$) to the water in the solar field heat exchanger is given by:

$$\dot{Q}_{HTF} = \dot{m}_{23}(h_{23} - h_{24}) \tag{10}$$

$$\dot{Q}_{water} = \dot{m}_{17}(h_{18} - h_{17}) \tag{11}$$

The exergy destruction rate in the solar field is calculated from:

$$\dot{I}_{SF} = \dot{X}_{SF,in} - \dot{X}_{SF,gain} \tag{12}$$

$$\dot{X}_{SF,gain} = \dot{X}_{23} - \dot{X}_{24} \tag{13}$$

$$\dot{X}_{SF,in} = \dot{Q}_{inc}[1 - \left(\frac{T_0}{T_{sun}}\right)] \tag{14}$$

where T_{sun} = the sun temperature which equals 5777 K.

The equation for the absorbed incident solar radiation as a function of DNI, incidence angle (θ), Incidence angle modifier and solar collectors' aperture area (A_{mirrors}) is:

$$\dot{Q}_{inc} = DNI * cos\theta * IAM * A_{mirrors} \tag{15}$$

where,

$$A_{mirrors} = N_{collectors} * W_{collectors} * L_{collectors} \tag{16}$$

The exergetic efficiency of the solar field is given by:

$$\eta_{II,SF} = \frac{\dot{X}_{SF,gain}}{\dot{X}_{SF,in}} \tag{17}$$

The ISCC as a whole

The exergy destruction rate in the cycle as a whole was obtained from:

$$\dot{I}_{ISCC} = \dot{I}_{compressor} + \dot{I}_{CC} + \dot{I}_{GT} + \dot{I}_{SF} + \dot{I}_{SFHex} + \dot{I}_{condenser} + \dot{I}_{CP} + \dot{I}_{FWP} + \dot{I}_{ST} + \dot{I}_{HRSG} + \dot{I}_{ExpValve1} + \dot{I}_{ExpValve2} + \dot{I}_{ExpValve3} \tag{18}$$

The exergetic efficiency of the ISCC is:

$$\eta_{II,Cycle} = \frac{\dot{W}_{elec,ISCC}}{\dot{X}_{ISCC,in}} \tag{19}$$

$$\dot{X}_{ISCC,in} = \dot{X}_{SF,in} + \dot{X}_{fuel} \tag{20}$$

RESULTS AND DISCUSSIONS

The software used to solve the equations is engineering equation solver (EES), developed by the University of Wisconsin Madison. The basic function provided by EES is the solution of a set of algebraic equations [12].

The exergy rates and other properties at each state point are presented in Table 3. These values were calculated for actual plant measured data (pressure, temperature, mass flow rate and DNI) on 28 August in Kuraymat at 2:00 PM (with DNI = 800 W/m^2). The gas turbine and steam turbine electric power output of 62.19 MW and 51.94 MW, respectively is obtained at the instance of recorded data with fuel consumption rate of 3.93 kg/s. The phase of each state point and the mass flow rates were illustrated in Table 3.

Results

The results showed that the overall thermal efficiency of the ISCC as a whole accounted as 32%. The rates of exergy destruction, percent of exergy destruction and the second law efficiency of the main components in the ISCC power plant, shown in Table 4, were calculated with data on Table 3.

The T-S diagram of the Kuraymat Rankine cycle for the previous measurements is shown in Fig. 2.

The exergy flow diagram, given as the percentage of total exergy input for the ISCC power plant is shown in Fig. 3. The figure reveals that the maximum exergy destruction occurs in the solar collector and the combustor.

Investigating the Sources of Exergy Destruction

Owing to the attained results, it is clear that amount of the exergy destruction in the various components of the ISCC is altered. This variation is supposed to be due to different reasons as the type of the device, the process, etc.

Table 3. Exergy rates and other properties at various locations of ISCCS, state numbers refer to Fig. 1. $\dot{X}$

State	**Fluid**	**Phase**	$\dot{m}$ *(kg/s)*	P *(bar)*	T *(˚C)*	h *(kJ/kg)*	s *(kJ/kg.K)*	$\dot{X}$ *(MW)*
dead state	Air	–	–	1.007	34.6	308.23	5.73	–
	water	liquid	–	1.007	34.6	145	0.5	–
	Oil	–	–	1.007	34.6	35.24	0.118	–
a	Fluegases	–	185.32	14.9	84.74	754.5	5.858	75.39
b	Fluegases	–	185.32	14.9	1288	1710.44	6.72	203.296
c	Fluegases	–	185.32	1.02	630.79	937.69	6.85	52.508
d	Fluegases	–	185.32	1.01	87.58	361.6	5.888	0.81
1	water	sat. liquid	49.01	0.08	38.36	160.6	0.5503	0.0004
2	water	liquid	49.01	9.36	38.94	163.9	0.5577	0.04738
3	water	liquid	49.01	1.2	38.94	163.6	0.5604	–
4	water	liquid	49.01	1.2	90	377	1.192	–
5	water	liquid	49.3	1.2	104.8	439.3	1.361	–
6	water	liquid	49.3	1.1	45.52	190.7	0.6453	3.998
7	water	liquid	49.3	140.08	58.78	257.8	0.8086	0.8723
8	water	liquid	49.3	137.1	165.67	707.8	1.984	5.229
8,a	water	liquid	45.73	137.1	165.67	707.8	1.984	4.85
8,b	water	liquid	3.57	133.06	165.67	707.8	1.984	0.3786
9	water	liquid	45.73	136.44	220.42	948.8	2.501	8.589
9,a	water	liquid	18.36	136.44	220.42	948.8	2.501	3.448
9,b	water	liquid	27.37	136.02	220.42	948.8	2.501	5.141
10	water	liquid	18.36	63.59	220.42	948.8	2.519	3.35
11	water	liquid	45.73	63.59	240.64	1041	2.701	4.006
12	water	sat. vapor	16.09	63	274.35	2785	5.898	17.971
13	water	superheated	43.46	65	277	1220	3.038	13.446
14	water	superheated	43.46	65	427.12	3237	6.594	55.638
15	water	superheated	43.46	65	474.64	3355	6.757	58.732
16	water	superheated	43.46	57.72	549.71	3542	7.048	63.192
17	water	liquid	27.37	64.85	220.4	948.8	2.518	4.996
18	water	superheated	27.37	64.85	279.34	2780	5.861	26.954
19	water	liquid	3.57	10.74	165.67	707.8	2.015	0.3438
20	water	sat. Vapor	4.37	10.74	183	2780	6.562	2.748
21	water	superheated	4.37	10.08	227.86	2892	6.822	2.86
21,a	water	superheated	2.1	9.97	227.86	2892	6.822	2.86
21,b	water	superheated	2.27	10.08	227.86	2892	6.822	2.86
22	water	sat.liq.vap.	49.01	0.08	32.6	2350	7.712	0
23	Oil	liquid	205	17	393	784.6	1.68	5.511
24	Oil	liquid	205	16.5	293	540.4	1.284	30.023
25	water	liquid	2742	1.01	28.81	120.8	0.42	0.6343
26	water	liquid	2742	1.05	28.81	120.8	0.42	0.6445
27	water	liquid	2742	1.013	38.26	160.3	0.5489	0.2493

Table 4. Exergy, percent of exergy destruction and the second law efficiency of different components of the ISCC.

Sub-System		$\dot{I}_{des}$ (kW)	$\dot{I}_{des}/\dot{I}_{total}$ (%)	η_{II} (%)
Solar Field	PTCs	69867	42.1	26.42
	Heat Exchanger	3131	1.89	94.79
Combined Cycle	Gas Turbine	7581	4.57	94.97
	Combustion Chamber	56369	34	78.29
	Air Compressor	7320	4.415	91.15
	Steam Turbine	9760	5.89	85.22
	Condenser	395.2	0.24	38.68
	Condensate Pump	112	0.0056	30
	Feed Water Pump	2477	1.5	25.15
	HRSG	8332	5.034	89.63
	Stack	810	0.489	–
ISCC Power plant		–	–	40.58

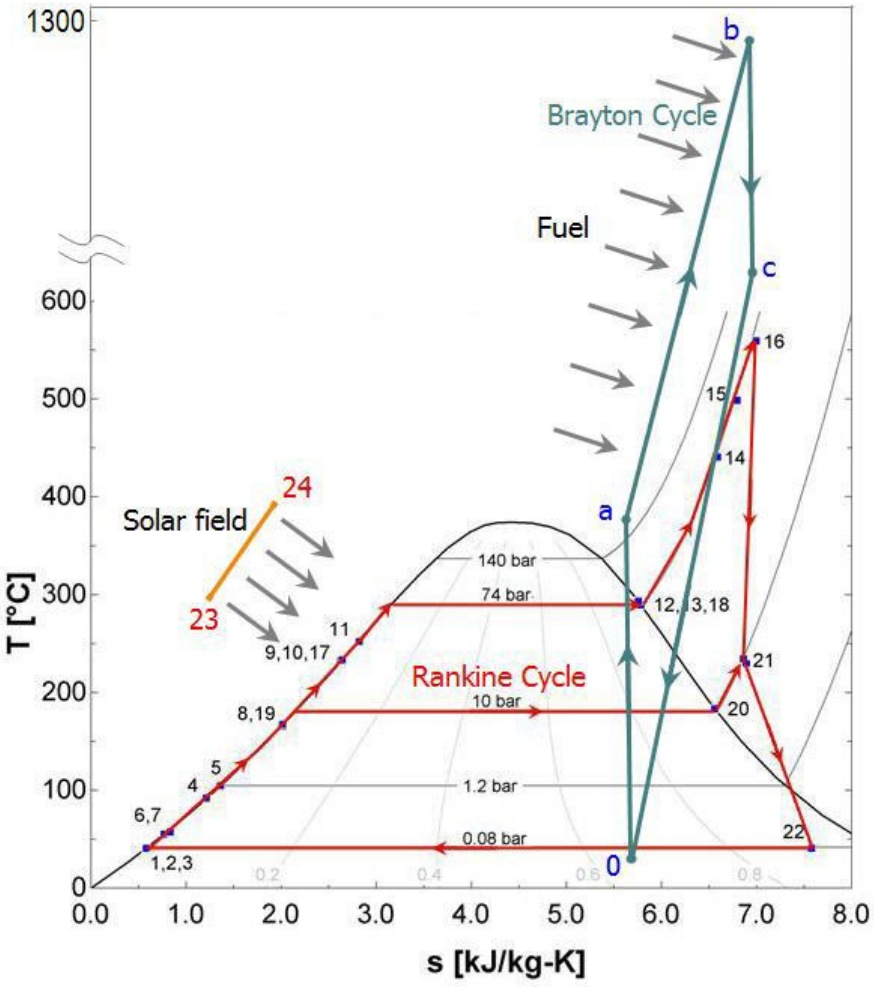

Fig. 2. The T - S diagram for Integrated Solar Combined Cycle, Egypt.

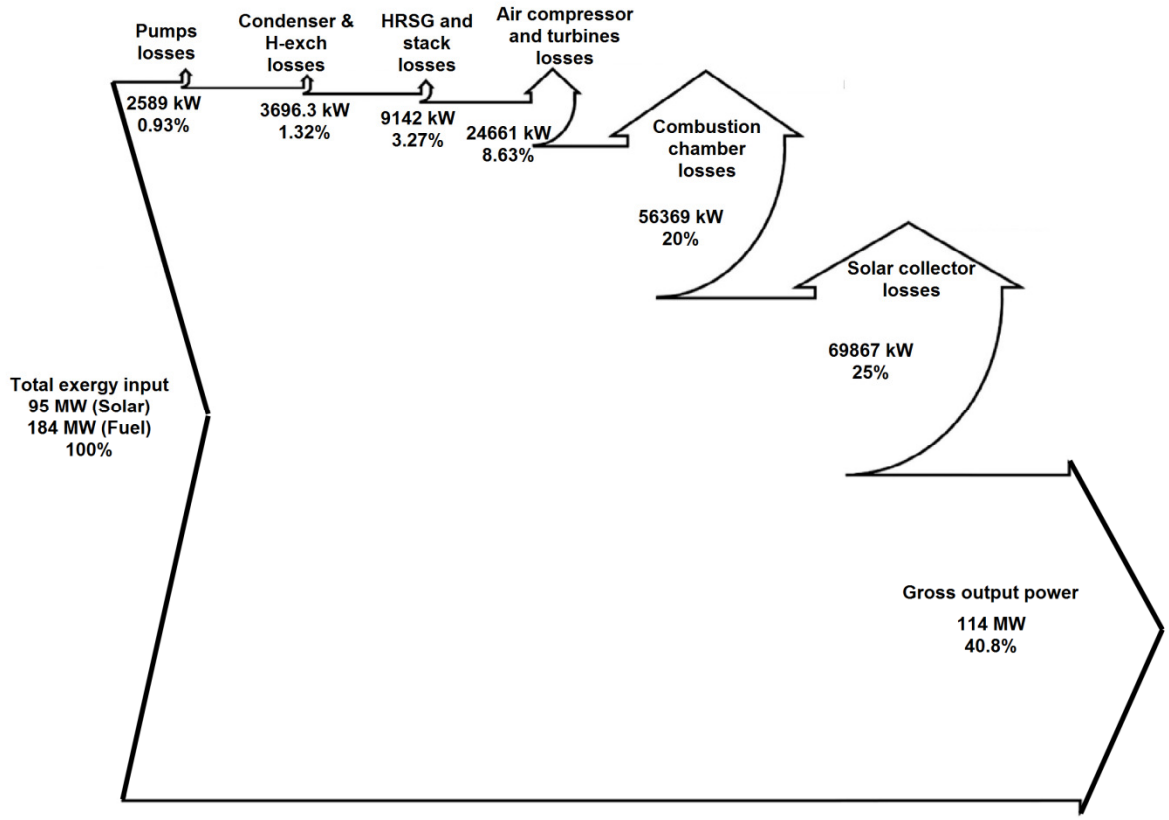

Fig. 3. Exergy flow diagram, given as the percentage of total exergy input for the ISCCS.

Moreover, it was disclosed that the combustion chamber and the solar field represent the sites of the highest exergy destruction in the ISCC. In this section, an attempt is done to explore and clarify the sources of exergy destruction in these two components in order to identify the possibility to enhance the performance of the components of major exergy destruction.

Irreversibilities in the combustion chamber

The combustion process is a really complex process. Thus, the entropy generation during the combustion process is rather high due to the complexity of that process. It was reported that oxidation of fuel during the combustion process utilizes around one over three of the usable fuel energy [13]. The combustion process includes diffusion, chemical reaction, heat transfer, friction and mixing and to implement all of these sub-processes, a considerable amount of the available energy is consumed. Most of this energy is unreachable (combustion activation energy, mixing, and diffusion).

There are three major physicochemical sub-processes responsible for entropy production during the combustion process [13]:

a) Diffusion of reactants (mixing of fuel and air molecules) and chemical reaction (fuel oxidation) where energy is consumed to overcome activation energy.
b) Heat transfer between combustion products and other neighbors of particles, this is called internal thermal energy exchange.
c) Mixing of combustion products with other constituents.

These processes cause exergy consumption (destruction) and thus results in a reduction in the system exergy.

All these processes destroy up to 40% of the useful exergy of the fuel. It was found that the dominant process of exergy destruction is the internal thermal energy exchange process.

On the other hand, it was found that more than 2/3 of the exergy destruction in combustion process occurs at the internal thermal exergy exchange process while fuel oxidation is responsible for up to 30% of the exergy destruction and the exergy destruction due to mixing process is about 3% of the total exergy destruction of the combustion process [13].

Many factors affect the exergy destruction in the combustion chamber. For example, the exergy destruction decreases with decreasing the excess air and increasing preheating temperature. Mixing at large temperature difference leads to high exergy destruction [14]. Also, the exergy destruction of the combustion chamber is affected by the molecular structure of the fuel where it increases with the chain length of the hydrocarbon [15].

The thermodynamic irreversible combustion process is path dependent. To get a quantitative solution for the total entropy production during the combustion process, correct information of the sequence of the combustion process and reactions must be offered.

The major exergy destruction in the combustion chamber occurs during the phase of internal thermal energy exchange between the system particles [13]. The unavoidability of the internal thermal energy exchange makes the possibility of reducing the exergy destruction during the combustion process is very difficult.
It was tried to avoid this heat transfer by introducing the concept of reversible combustion where it was proposed theoretically to preheat the reactants to the equilibrium temperature and partial pressures without reaction but it couldn't be achieved practically [13].

Irreversibilities in the solar field
Exergy is destructed and lost in the solar field. The exergy destruction is due to heat transfer between the sun and the absorber, heat transfer between the absorber and the HTF and the friction of the viscous HTF. The exergy loss is due to the optical efficiency (the ratio of sunlight capture to incident sunlight) and the heat transfer to the surrounding.

The solar collector is considered to be the main source of exergy destruction in the solar field due to the high-temperature difference in the collector. The major contribution of the exergy destruction in the solar collector is due to the heat transfer between the sun and the absorber, while the major exergy loss occurs due to optical errors [16].

It was reported that the exergy destruction due to heat transfer between the sun and the absorber accounts for 35% to 40% of the total exergy destructed. Exergy losses to the surrounding accounts for 5% to 10% of the total exergy destructed [16].

It is thought that to decrease the exergy losses from the solar collector (i.e. increase the collector energetic efficiency) attention should be pointed to improve the optical parameters (as mirror reflectivity, the transmissivity of the glass envelope, the

absorptivity of the HCE selective coating and focal length of the collectors etc...) of the collector.

Regards the exergy destruction due to heat transfer, the opportunity of improving that part may face great challenges because of the existence of the finite temperature differences; which is essential for the heat transfer process and cannot be avoided.

CONCLUSIONS

The objective of this study is to evaluate the performance of an existing 135MW ISCC power plant in Kuraymat; Egypt. The ISCC was thermodynamically studied under Egypt climatic conditions. The integration of the solar energy into the NGCC was analyzed as power-boosting mode. A mathematical model was developed to investigate the performance of the solar field [17]. Energy and exergy analysis for the ISCC power plant were performed to identify the causes and locations of the highest thermodynamic irreversibilities. The main conclusions of this study are:

- The solar field has the lowest exergetic efficiency in the cycle.
- The combustion chamber and the solar field have the highest exergy destruction percentage among all subsystems.
- Major portion of CC exergy destruction is unavoidable.
- Exergy destruction in Solar Field is a complicated process.
- Tremendous effort in direction of science needed to improve the utility of the solar energy.

REFERENCES

[1] M. Geyer *et al.*, “Trough integration into power plants—a study on the performance and economy of integrated solar combined cycle systems”, *Energy*, vol. 29, no. 5–6, pp. 947–959 (2004).

[2] The World Bank Report, “The World Bank Report No : ICR2173 Implementation Completion and Results Report on a Grant in the Amount of US$ 49.80 Million to The Arab Republic of Egypt for the Kureimat Solar Thermal Hybrid Project”, (2012).

[3] O. Behar, A. Kellaf, K. Mohamedi, and M. Belhamel, “Instantaneous performance of the first Integrated Solar Combined Cycle System in Algeria”, *Energy Procedia*, vol. 6, pp. 185–193 (2011).

[4] A. Baghernejad and M. Yaghoubi, “Exergy analysis of an integrated solar combined cycle system”, *Renew. Energy*, vol. 35, no. 10, pp. 2157–2164 (2010).

[5] G. Brakmann, F. A. Mohammad, M. Dolejsi, and M. Wiemann, “Construction of the ISCC Kuraymat”, *International SolarPACES Conference 2009*, no. 5, pp. 1–8 (2009).

[6] Eastman, “Selection Guide High-performance fluids for precise temperature control”, p. 10.

[7] SOLUTIA, “THERMINOL VP-1 Heat Transfer Fluid”, *Data sheet*, p. 7.

[8] FLAGSOL Company, “Performance Test Procedure,” 2010.

[9] J. Ramachandran and M. C. Conway, “MS6001FA – An Advanced-Technology 70-MW Class 50/60... Hz Gas Turbine”, *Tech. Doc. GER-3765B GE Power Syst. Schenectady, NY*, p. 14, 1996.

[10] A. Rashad and A. El-Maihy, “Energy and Exergy Analysis of a Steam Power Plant in Egypt”, *Aerospace Science and Aviation Technology (ASAT-13)* (2009).
[11] T. J. Kotas, *The Exergy Method of Thermal Plant Analysis*, 1st ed. London, UK: Anchor Brendon Ltd, Tiptree, Essex (1985).
[12] S. A. Klein and G. Nellis, *Mastering EES*. (2012).
[13] W. R. DUNBAR and N. LlOR, “Sources of Combustion Irreversibility”, *combust. Sci. Tech.*, vol. 103, pp. 41–61 (1994).
[14] H. Athari, S. Soltani, M. A. Rosen, S. M. Seyed Mahmoudi, and T. Morosuk, “Comparative exergoeconomic analyses of gas turbine steam injection cycles with and without fogging inlet cooling”, *Sustain.*, vol. 7, no. 9, pp. 12236–12257 (2015).
[15] M. Anheden, “Analysis of gas turbine systems for sustainable energy conversion”, Royal Institute of Technology (2000).
[16] R. V. Padilla, A. Fontalvo, G. Demirkaya, A. Martinez, and A. G. Quiroga, “Exergy analysis of parabolic trough solar receiver”, *Appl. Therm. Eng.*, vol. 67, no. 1–2, pp. 579–586, 2014.
[17] A. Temraz, A. Elweteedy, A. Rashad, and K. AlShazly, “Seasonal Performance Evaluation of ISCCS Solar Field in Kureimat, Egypt”, *6th Annual International Conference on Sustainable Energy and Environmental Sciences (SEES 2017)*, no. March, pp. 1–8 (2017).